Appl Phys A (2013) 112:165–171
DOI 10.1007/s00339-012-7229-3

Applied Physics A
Materials Science & Processing

Interferometric determination of the high-intensity laser-pulse-material interaction site

Tomaž Požar · Peter Gregorčič · Janez Možina

Received: 20 July 2011 / Published online: 11 September 2012

Abstract We developed a method that accurately determines an unknown position of the high-intensity laser-pulse-material interaction site on the front side of a plate. It is based on interferometric measurements of a normal displacement at known positions on the plate's rear side. The displacement is caused by reflections of various pulsed-laser-induced mechanical waves. We have superseded the long-established time-of-flight approach with the improved, triple-echo method. To accurately locate the origin of the laser-induced ultrasound on the plate with a known thickness, we only need to detect the arrivals of the first three consecutive mode unconverted waves. Our method works without knowing the propagation velocities of various ultrasonic waves and additionally solves some time-related drawbacks of the conventional time-of-flight approach. The relative uncertainty of the measured source-receiver separations obtained with the presented method is less than 0.01.

1 Introduction

A plate is the most commonly encountered work-piece geometry in laser materials processing. Often, accurate knowledge of the position of the interaction site [1], where laser pulse illuminates the surface of the plate, cannot be determined in advance, especially when the illuminated solid plate is covered with transparent media. Such experimental conditions are common in laser shock peening where a typical energy of several joules is deposited within few nanoseconds in a confined ablation regime [2, 3].

T. Požar (✉) · P. Gregorčič · J. Možina
Faculty of Mechanical Engineering, University of Ljubljana, Aškerčeva 6, 1000 Ljubljana, Slovenia
e-mail: tomaz.pozar@fs.uni-lj.si

Online monitoring of the laser-pulse-material interaction site from the same side of the plate is often difficult, because ablated material is expelled from the surface of the processed material [4]. This may damage nearby sensors or stain the monitoring optics. The processed surface may also be covered with liquids [2, 3]. This aggravates the use of contacting sensors. Additionally, high-intensity laser-pulse-material interaction is always accompanied by a plasma plume. Plasma radiates visible light, which due to its wide spectrum, cannot be filtered, and thus saturates optical detectors.

High-intensity light-material interaction induces high-amplitude and high-frequency ultrasonic mechanical waves [5]. We describe how the relative position of each processing laser pulse on the front side of the plate can be determined by measuring displacements at its rear side with a homodyne quadrature laser interferometer [6]. These displacements, with amplitudes that can exceed 100 nm, are caused by multiple rebounds of the laser-induced ultrasonic waves.

In addition to monitoring laser-material processing, great interest in the determination of the source-receiver separation on a plate also originates from the field of acoustic emission [7, 8]. This distance is obtained by evaluating waveforms corresponding to the arrivals of the dispersive Rayleigh–Lamb waves in the far-field, i.e., for distances much greater than the thickness of the plate h. This method is fairly inaccurate with absolute uncertainty of a few h [9]. In contrast, our novel, triple-echo method, presented in this paper, is suitable for accurate determination of the high-intensity laser-pulse-material interaction site in the near-field, for distances smaller than $10h$. We achieved an absolute uncertainty of less than $0.01h$.

In this paper, we first shortly review the principle of source location, exposing the major disadvantages of the conventional time-of-flight (ToF) triangulation approach [7, 8, 10]. Then we introduce an enhanced ToF method that efficiently solves the aforementioned drawbacks. This approach is explained in detail together with its limitations, improved accuracy over the conventional approach, and possible extensions for other applications, such as: determination of the plate's thickness [11] and the depth of the laser-induced damage spot inside a transparent plate [12]. Then we develop a special case of the enhanced ToF method, called the triple-echo method. This triangulation method is suitable to extract the information about the high-intensity laser-pulse-material interaction site on a plate. Two measured displacement waveforms are analyzed. The first is measured with the shortest source-receiver separation. This one is used to obtain some basic knowledge of the temporal shape of the force function that models the generation of the ultrasound. The second displacement waveform is obtained with an unknown separation of the source and the receiver. This distance is then evaluated using the presented triple-echo method. A line-tracking experiment was performed to validate the ability of our method to follow the laser-pulse-material interaction site as it moves on the surface of the plate.

2 Source location principle

2.1 Conventional ToF method

An unknown position of a laser-induced, ultrasonic point-source on the plate's surface $\mathbf{R}_0 = (x_0, y_0)$ can be unambiguously determined if at least 3 distance-measuring point receivers are placed on either of the plate's surfaces at known, noncollinear positions $\mathbf{R}_i = (x_i, y_i), i = 1, 2, 3 \ldots$.

In ultrasonic source localization techniques [7, 8, 10], the distance from the source to each receiver $r_i = |\mathbf{R}_i - \mathbf{R}_0| = c(t_i - t_0)$ is inferred by measuring the arrival times of ultrasonic waves at each receiver t_i and by knowing in advance the velocity of the ultrasonic disturbance c and the time of the initiation of ultrasound t_0. The time difference $t_i - t_0$ is called the time-of-flight (ToF). Often, the value of c is known with poor accuracy and the time when the event takes place t_0 can be completely unknown. This demands a deployment of at least 5 detectors, as will be shown below, thus limiting the applicability of the conventional ToF method.

When the unknown coordinates of the source (x_0, y_0) are inferred from the arrival times t_i of ultrasonic waves at known locations (x_i, y_i), the following systems of equations

$$r_i^2 = c^2(t_i - t_0)^2 = (x_i - x_0)^2 + (y_i - y_0)^2, \qquad (1)$$

needs to be solved.

Consider first that only 2 detectors were used, and that we have already obtained the distances r_1 and r_2 from arrival times t_i either by knowing both c and t_0 in advance or by a method that is independent of c and t_0. Geometrically, we can now draw 2 circles with radii r_1 and r_2 centered at the 2 receivers. The intersection of the two circles takes place at two points (the two solutions of Eqs. (1) for $i = 1, 2$); one of which is the true position of the source while the other is it mirror image. Often, the mirror image can be discarded, because it is either out of the plate or at an unexpected location. In the case of ambiguity, a third detector is required to obtain the correct location of the source by picking out one of the two solutions of Eqs. (1) for $i = 1, 2$, which coincides with one of the two solutions of Eqs. (1) for either $i = 2, 3$ or $i = 1, 3$. Beside this circle method, a hyperbola method based on arrival time differences in often used when t_0 is unknown [10].

If additionally to the unknown location of the source, c and t_0 are also not known, then at least 4 receivers are needed to solve for four unknowns (x_0, y_0, t_0, c). But for $i = 1, 2, 3, 4$, the system of Eqs. (1) yields 3 possible solutions that satisfy the condition $c > 0$. Again, another detector is required to pinpoint the location of the source unambiguously.

The described approach, based on the conventional ToF method, has three major drawbacks. They either limit the accuracy of the calculated position of the source when the velocity of propagation of ultrasonic waves c and the ToFs $(t_i - t_0)$ are known with poor accuracy or demand the use of additional receivers if the same parameters are completely unknown. First, the initiation time of ultrasound t_0 cannot be accurately determined due to triggering, electronic and optical delays in the detection system, or cannot be determined at all if triggering to the event is not possible. Second, the shape of the signal corresponding to the reflection of the ultrasonic wave is rather wide. Therefore, one needs to decide where on the signal one will measure the arrival time. This ambiguity directly affects the value of the resulting position through the value of the measured ToF. Third, the velocity of the ultrasonic wave c is often given with poor accuracy.

2.2 Enhanced ToF method

We will show how to eliminate the previously described disadvantages of the conventional ToF method by taking into account the geometry of the medium of propagation. We will present an enhanced ToF method that is independent of the velocity of the ultrasonic disturbance c and the time of the initiation of ultrasound t_0. It can be used on elastic, homogeneous, and isotropic parallel-sided plates with known thicknesses and gives the source-receiver separation r from a single surface-displacement measurement.

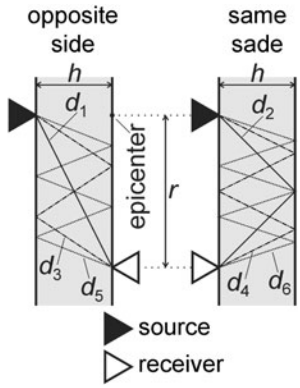

Fig. 1 Cross-section schemes of the source location. The source and the receiver can be on opposite sides (left-hand side sketch) or on the same side (right-hand side sketch) of the plate. The wave-propagation rays are shown for the first three arrivals (triple-echo) at the location of the receiver

We assume that bulk waves, either the longitudinal P-wave or the transversal S-wave, the conical head wave (H-wave), and the Rayleigh surface wave are generated by a normal force acting at a point on the plate's surface at the time t_0. This short-lasting normal force satisfactory models the generation of ultrasound in the ablative regime. The shortest the time duration of the force, the more localized are the propagating waves, and consequently, the more pronounced and easily discerned are their fingerprints in the detected waveform.

Different types of laser-induced ultrasonic bulk waves propagate with different velocities spherically away from the source. When they reach the plate's boundaries, they are reflected and confined within the plate. At each reflection, the incoming P-wave may be converted not only into a reflected P-wave, but also into a reflected, mode converted S-wave. Similar mode conversion may occur at the reflection of the S-wave. For the purpose of an accurate source location, we are interested mainly in the pure waves. These can be either S- or P-waves that have never mode converted during their entire path from the source to the receiver. The property of the pure waves that we take advantage of, is their constant velocity of propagation c. The receiver detects the nth reflection of the pure wave at the time

$$t_n(n,h,r,c,t_0) = \frac{d_n}{c} + t_0. \tag{2}$$

This time depends on the number of reflections n, the thickness of the plate h, the relative distance between the source, and the receiver r (see Fig. 1), the velocity of propagation c (c_P for the P-wave and c_S for the S-wave), and the initiation-time of the ultrasound t_0. The distance

$$d_n(n,h,r) = n\left[h^2 + \left(\frac{r}{n}\right)^2\right]^{1/2} = h\left(\xi^2 + n^2\right)^{1/2} \tag{3}$$

can be geometrically derived from Fig. 1. This distance is the length of the generalized ray which corresponds to the path traveled by the wavefront of the pure wave. In Eq. (3), ξ is a dimensionless variable defined as the ratio between r and h. As seen in Fig. 1, n is a positive odd integer when the source and the probe are on opposite surfaces of the plate while n is an even integer when they are on the same side of the plate. Here, $n = 0$ corresponds to the source-receiver separation $d_0 = r$ along the surface of the plate.

First, we shall solve the problem of the inaccurate knowledge of the ultrasound-initiation time t_0. We can get rid of this free parameter by subtracting two different arrival times of the same pure wave on a single waveform.

$$\Delta t_{(m,n)}(m,n,h,r,c) = t_m - t_n = \frac{1}{c}(d_m - d_n). \tag{4}$$

Then we shall make a ratio η of two such time intervals in order to divide out the velocity of propagation c, and thus solve the second problem of the conventional ToF approach.

$$\begin{aligned}\eta(m,n,p,q,\xi) &= \frac{\Delta t_{(m,n)}}{\Delta t_{(p,q)}} = \frac{t_m - t_n}{t_p - t_q} = \frac{d_m - d_n}{d_p - d_q} \\ &= \frac{(\xi^2+m^2)^{1/2} - (\xi^2+n^2)^{1/2}}{(\xi^2+p^2)^{1/2} - (\xi^2+q^2)^{1/2}}.\end{aligned} \tag{5}$$

This can only be done if we detect at least three different echoes of the same pure wave. The nondimensional ratio η is now dependent only on the reflection indices m, n, p, and q and the ratio ξ between the projection of source-receiver distance to the plate's surface r and the plate's thickness h. Note that the ratio η is independent of c and t_0. Once we calculate η using the measured values of $\Delta t_{(m,n)}$ and $\Delta t_{(p,q)}$ from a single waveform, we can solve Eq. (5) to obtain ξ. In general, the inversion of Eq. (5) cannot be expressed in a closed form.

The last deficiency of the conventional ToF method lies in the fact that the measured arrival time depends on the choice of the position of the arrival time on a rather wide signal-pulse shape. Here, we rather rely on the position-independent determination of the time intervals $\Delta t_{(m,n)} = t_m - t_n$, appearing in Eq. (5), by comparing similar features in the displacement waveform corresponding to the echoes of the pure waves. The time interval is obtained from the displacement waveform using the cross-correlation procedure [13]. This is a robust method to determine the time delay between two selected wave-arrivals by comparing the whole arrival-signal shapes rather than extremes or other positions on the signal.

Clearly, the sought distance $r = h\xi$ depends on the plate's thickness h and on ξ which can be extracted numerically from Eq. (5). Both, h and η have to be measured. The measurement of h is straightforward. Experimentally, we determine h with an uncertainty of δh and the time intervals $\Delta t_{(m,n)}$ and $\Delta t_{(p,q)}$ with an uncertainty of δt. The relative uncertainty of the sought distance r is evaluated as follows:

$$r\left(1 \pm \frac{\delta r}{r}\right) = h\xi\left(1 \pm \left[\frac{\delta h}{h} + \frac{\delta \xi}{\xi}\right]\right)$$
$$= h\xi\left(1 \pm \left[\frac{\delta h}{h} + \left\{\frac{\mathrm{d}\xi}{\mathrm{d}\eta}\frac{\eta}{\xi}\right\}\frac{\delta \eta}{\eta}\right]\right)$$
$$= h\xi(\eta)\left(1 \pm \left[\frac{\delta h}{h} + \left\{\frac{\mathrm{d}\xi(x)}{\mathrm{d}x}\bigg|_{x=\eta}\frac{\eta}{\xi(\eta)}\right\}\right.\right.$$
$$\left.\left.\times\left(\frac{\delta t}{\Delta t_{(m,n)}} + \frac{\delta t}{\Delta t_{(p,q)}}\right)\right]\right). \quad (6)$$

Thus, the location of an unknown position of the ultrasonic source on the front side of the plate with a known thickness can be accurately determined with the known position of the receiver on either of the plate's sides using the triple-echo method. This method works as long as we are able to measure the elapsed time of at least three reverberations of the same, laser-generated, pure ultrasonic bulk wave.

Moreover, our enhanced ToF method can be slightly modified to determine the depth of the laser-induced damage spot inside a transparent parallel-sided plate. A focused laser pulse of sufficient energy and peak power that surpasses the bulk damage threshold can cause a breakdown, leaving behind a permanent damage. When the damage occurs, mechanical waves are released and can be used to infer the location of the damage spot.

Imagine the point source in the left-hand side sketch in Fig. 1 to be buried within the plate at the depth h_D below the place, where the laser-pulse perpendicularly enters the plate. In this case, Eq. (3) is altered to

$$d_n(n, h, \xi, z) = \begin{cases} n[\xi^2 + (n-z)^2]^{1/2} & n \text{ odd} \\ n[\xi^2 + (n-1+z)^2]^{1/2} & n \text{ even,} \end{cases} \quad (7)$$

introducing an additional normalized variable $z = h_\mathrm{D}/h$. The remaining steps of the derivation of the enhanced ToF method for the buried source are identical to the case, where the source lies on the surface of the plate, only this time one needs to solve

$$\eta(m, n, p, q, \xi, z) = \frac{t_m - t_n}{t_p - t_q} = \frac{d_m - d_n}{d_p - d_q} \quad (8)$$

for z. To determine the depth of the damage spot $h_\mathrm{D} = hz$, the separation $r = h\xi$ between the receiver and the entering point of the laser pulse on the plate's surface must be known in advance additionally to the plate thickness h and the measured value of η.

2.3 Triple-echo method

In the previous subsection, we developed a general method. However, from now on, we will limit ourselves to the special case, where the source and the receiver are on the opposite sides of the plate. Additionally, we will consider only the first three reflections of a pure P-wave, i.e., P, 3P, and 5P. For this reason, we call this approach the *triple-echo method*. Here, the ratio η can be expressed as

$$\eta(\xi) = \frac{\Delta t_{(5,3)\mathrm{P}}}{\Delta t_{(3,1)\mathrm{P}}} = \frac{(\xi^2+25)^{1/2} - (\xi^2+9)^{1/2}}{(\xi^2+9)^{1/2} - (\xi^2+1)^{1/2}}. \quad (9)$$

Equation (9), which is a special case of a more general Eq. (5), can be inverted analytically. We find:

$$r(h, \eta) = h\xi(\eta)$$
$$= h\left[-\frac{(\eta+4)(\eta+2)(2\eta-1)(\eta-1)}{(\eta+1)\eta(\eta-2)}\right]^{1/2}. \quad (10)$$

Figure 2 shows the function $\xi(\eta)$ (the solid black curve) and the ratio of relative uncertainties $\kappa(\eta)$ (the dashed black curve)

$$\kappa(\eta) = \frac{\delta\xi/\xi}{\delta\eta/\eta} \doteq \frac{\mathrm{d}\xi}{\mathrm{d}\eta}\frac{\eta}{\xi} \quad (11)$$

for $1 \le \eta < 2$. As seen in Fig. 2, the ratio κ rapidly increases near the epicenter ($\eta < 1.1$; the solid gray lines) and in the far field ($\eta > 1.8$; the solid gray lines) limiting the accuracy of the triple-echo method for practical purposes in the annulus defined by $1 < \xi < 7$ or $h < r < 7h$. The location of the source can thus be accurately measured inside this circular area where $3 < \kappa < 6.5$ (the horizontal dashed gray lines).

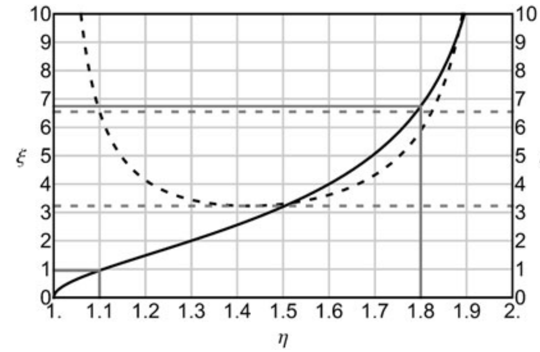

Fig. 2 Normalized distance ξ (the *solid black curve*) and the ratio of relative uncertainties κ (the *dashed black curve*) as a function of the measured ratio of time intervals η obtained from the first three arrivals of the pure wave

At certain values of $\xi = r/h$, the waves interchange their place in their chronological order of arrival times at the detector. The first wave arriving at the location of the receiver is always the P-wave that has traveled along the straight line from the source. Later arrival times, in general, depend on material properties. For a 10-mm-thick Al plate, the arrival times of interest for the location determination using the triple-echo method are shown in Fig. 3. They are calculated

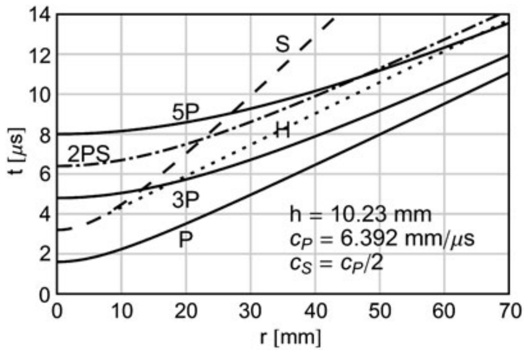

Fig. 3 Calculated wave-arrival times t as a function of the distance r from the receiver to the epicenter for an Al plate

as a function of r, the distance which we want to determine by measurement. As seen in Fig. 3, the S- and H-wave arrivals coincide with the 3P-wave at about $r = 13.2$ mm and 17.7 mm, respectively. Similarly, S-, 2PS- and H-wave coincide with the 5P-wave at about $r = 27.1$ mm, 47.0 mm and 65.0 mm, respectively. Further than 65.0 mm away from the epicenter, the first three consecutive pure P-wave arrivals are no longer disturbed by other waves. As found out by our measurements, pure P-waves can be clearly distinguished from the waveform when their arrival times coincides with the H-wave, while synchronous arrivals of S- or 2PS- with the pure P-wave affects accurate determination of the P-wave arrival time.

3 Results

3.1 Epicentral displacement

Some properties of an ultrasonic source accompanying high-intensity laser-pulse-matter interaction can be extracted from the displacement measured at the epicenter. Epicenter is the position closest to the source but on the other side of the plate. One of such properties is a temporal distribution of the normal force that generates the transient ultrasonic displacement field.

Based on the epicentral displacement, the velocity of the P-wave can also be determined very accurately from multiple reverberations of the pure P-wave. Moreover, the analysis of the time delay between successive pure P-wave reverberations can be used to align the processing beam and detection beam forming a perfect epicentral geometry with coaxial beams.

We employed a Q-switched Nd:YAG processing laser with a top-hat pulse. The pulse has a 10 ns FWHM duration and a wavelength of 1064 nm. Its exiting diameter is 8 mm and carries a maximum energy of 1.6 J. It is then focused normally on the plate using a positive lens with a

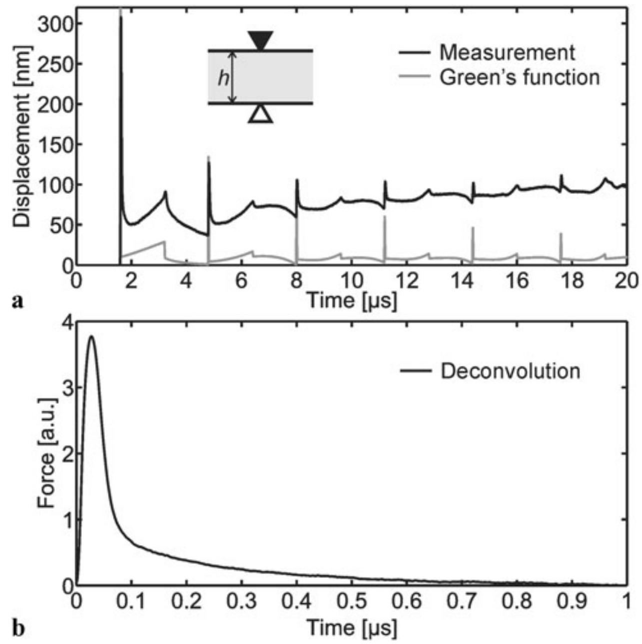

Fig. 4 (**a**) Epicentral normal displacement caused by an intense laser-induced ultrasound in a 10-mm-thick Al plate measured with an interferometer (the *black curve*) and the corresponding theoretical normal-impulse response (the *gray curve*). (**b**) Time distribution of the normal force obtained with the method of deconvolution

100-mm focus length. The pulse-intensity on the plate surface is above 10^{10} W/cm^2 but kept below the air-breakdown intensity threshold.

Figure 4a shows the epicentral displacement measured with a homodyne quadrature laser interferometer (the black curve) and the theoretical normal-normal impulse response—the Green's function—(the gray curve) [14] for a 10-mm thick Al plate. The more reverberations of the pure P-wave one can discern from the near epicentral displacement waveform, the more accurate the value of its propagation velocity can be measured. This is because when the source and receiver are not exactly above each other, the ray of the initial P-wave travels a little longer path compared to the thickness of the plate. With each reflection of the pure P-wave, this path gets more and more perpendicular to the plates boundaries until we can no longer see it changing due to the limited resolution of our measurement. From the measurement in Fig. 4a, we obtained $\Delta t_{(9,7)P} = 3.2001$ μs and $\Delta t_{(11,9)P} = 3.1999$ μs, which tells us that the absolute uncertainty of the echo-time is below 1 ns. The calculated longitudinal velocity is $c_P = 2h/\Delta t_{(11,9)P} = 6.400(1 \pm 0.002)$ mm/μs and its accuracy is primarily affected by the relative uncertainty of the measured thickness of the plate.

The Green's function was calculated with the following input parameters: $h = 10.23$ mm, $c_P = 6.394$ mm/μs and $c_S = c_P/2$. It is clear from Fig. 4a that Green's function has similar features as the measurement. Using both, the measurement and the Green's function, we evaluated the temporal distribution of the normal force with a direct time-domain deconvolution (see Fig. 4b). It can be deduced that the shape of the forcing function in the intense ablative regime is composed of the some 10-ns FWHM pulse similar to the time-distribution of the laser-pulse power followed by an about 100 times longer, slowly decreasing tail [15]. Such force thus generates well localized ultrasonic waves that can be easily discriminated in the displacement waveform which is a requirement of the triple-echo method.

3.2 Location of the interaction site

To demonstrate how we can determine the high-intensity laser-pulse-material interaction site based on the normal displacement measurement obtained with an interferometer, we present the results where the measuring beam of the interferometer is about $2h$ from the epicenter. The detected displacement in the first 10 μs is presented in Fig. 5. The consecutive order of wave-arrivals for $r \approx 2h$ is: P, 3P, H, S, 2PS, 5P, P2S. Only the first three clearly distinguishable pure P-waves (P, 3P, and 5P) are used in the triple-echo method to obtain the sought distance r.

The two time intervals, $\Delta t_{(3,1)P} = 2.818$ μs and $\Delta t_{(5,3)P} = 2.139$ μs, are obtained from the interferometer's output using the cross-correlation procedure. We managed to determine a time interval with an uncertainty of $\delta t = 1$ ns. The thickness of the plate was measured at 10 different positions on the plate with a digital caliper used as the reference method. The resulting mean thickness was $h = 10.23$ mm with a standard deviation of $\delta h = 0.02$ mm. Inserting the measured time intervals and the thickness of the plate in Eqs. (6), (9)–(11), we obtain $r = 21.4\ (1 \pm 0.005)$ mm.

We compared this value with the distance between the two markings that the laser pulses left behind; one in the epicentral position and the other at an unknown position determined above. The centers of the markings were displaced by 21.2 (1 ± 0.01) mm as measured by a digital caliper. This independent measurement agrees well with the interferometric result in the range of uncertainty interval.

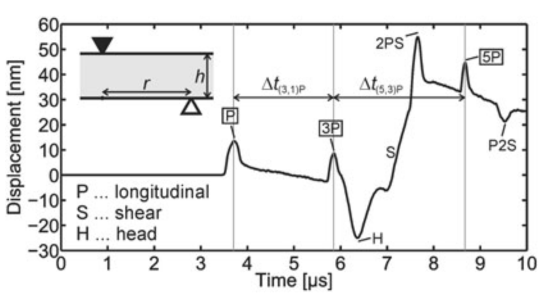

Fig. 5 The measured off-epicentral normal displacement caused by an intense laser-induced ultrasound in a 10-mm-thick Al plate is used to determine the distance r from the detector to the epicenter. The arrival times of the P, 3P, and 5P waves are used in the triple-echo method

To further demonstrate the capability of the presented method to localize the high-intensity laser-pulse-material interaction site, we performed a line-tracking experiment. The measuring beam of the interferometer was set in the epicentral position. This position was found with the procedure described in Sect. 3.1. Then single laser-pulses ablated the front side of the plate from the epicentral position to $r = 70$ mm leaving behind 141 equidistant marks with a mark-to-mark separation of 0.2 mm. For each laser-pulse, a displacement history similar to the one presented in Fig. 5 was recorded. The source-receiver separation was then obtained from the waveform using the triple-echo method. The differences r_r from the epicentral mark to all the other marks were again measured with the reference method and compared with the separations r_m obtained with the triple-echo method. It was found that from $r = 10$ mm to $r = 70$ mm, the relative error $(r_r - r_m)/r_r$ was always below 0.01. Unfortunately, we were unable to determine the source-receiver separation with the triple-echo method whenever the arrivals of the S- or 2PS-waves coincided with the pure P-wave. When such synchronous arrivals occur (see Fig. 3), conventional ToF method must be employed. Note that when the conventional ToF method is used, the source-receiver separation cannot be obtained from a single waveform without knowing the velocity of propagation of the direct P-wave c_P and the onset time of ablation t_0.

With a similar line-tracking experiment performed from $r = 20$ mm to $r = 22$ mm with a mark-to-mark separation of 0.1 mm, we showed that source-receiver separation determination based on the triple-echo method distinguishes two laser-pulse-material interaction sites that are separated by 0.1 mm in the direction radially away from the epicenter. For comparison, to achieve the same accuracy with the conventional ToF method, assuming the value of $(t_1 - t_0)$ is known and has negligible uncertainty, and that the only uncertainty in the measured r is due to inaccurate knowledge of c_P, one would have to know in advance the value of c_P with a relative uncertainty of $\delta c_P = (r\delta r)/(d_1(t_1 - t_0)) = 0.004$. This implies that for a given plate, c_P needs to be measured with a relative accuracy of a few per mille before a conventional ToF method can be used to infer the source-receiver separation with comparable accuracy. Independence of the triple-echo method on the value of wave-propagation velocity c and on the initiation time of ultrasound t_0 is therefore crucial for the accurate determination of source-receiver separation.

4 Conclusion

We experimentally demonstrated that an unknown location of the high-intensity laser-pulse-material interaction site on a front side of a plate with a known thickness can be accurately determined from the displacement waveforms measured at least three known positions on the plate's rear side.

Here, the near field normal displacement was measured using a homodyne quadrature laser interferometer. The ultrasound was generated with a Q-switched pulse with intensity larger than 10^{10} W/cm^2. Such an intense ablative regime is commonly encountered in laser shock peening.

The source-receiver separation was determined with an enhanced ToF method, called the triple-echo method. This novel method is useful as long as the time elapsed between the consecutive three reverberations of the same, laser-generated, pure ultrasonic bulk wave can be extracted from the displacement waveform. The smallest uncertainty of the measured source-receiver separation r, evaluated with a triple-echo method, is obtained when $h < r < 7h$. This measurement is independent of the velocity of propagation of various laser-induced waves and on the initiation time of ultrasound. Time delays between consecutive pure wave arrivals were accurately measured with a cross-correlation method. Our measurements point out that the achieved absolute uncertainty of the measured source-receiver separation on a 10-mm Al plate is 0.1 mm when the separation is about 20 mm. The proposed method reduces the number of receivers from 3 to 1 when the source-receiver distance has to be extracted from the displacement waveform without prior knowledge of the velocity of propagation of ultrasonic waves and of the beginning of the ultrasound-emitting event.

The enhanced ToF method can also be employed to accurately measure an unknown thickness of the plate if both the position of the source and the detector are known in advance regardless if the source, and the detector are on the same or opposite sides of the plate. Moreover, an extension of this method allows for the localization of the depth of the laser-induced damage spot inside a transparent plate.

References

1. N.N. Hsu, S.C. Hardy, in *Elastic Waves and Non-Destructive Testing of Materials*, vol. 29, ed. by H.-Y. Pao (The American Society of Mechanical Engineers, San Francisco, 1987), p. 85
2. L. Berthe, R. Fabbro, P. Peyre, L. Tollier, E. Bartnicki, J. Appl. Phys. **82**, 2826 (1997)
3. K. Ding, L. Ye, *Laser Shock Peening: Performance and Process Simulation* (CRC Press, Boca Raton, 2006)
4. W.M. Steen, J. Mazumder, *Laser Material Processing* (Springer, London, 2010)
5. T. Požar, P. Gregorčič, J. Možina, Opt. Express **17**, 22906 (2009)
6. P. Gregorčič, T. Požar, J. Možina, Opt. Express **17**, 16322 (2009)
7. R.K. Miller, M.F. Carlos, R.D. Finlayson, V. Godinez-Azcuaga, M.R. Rhodes, F. Shu, W.D. Wang, in *Nondestructive Testing Handbook—Acoustic Emission Testing, Chap. 4: Acoustic Emission Source Location*, vol. 121, ed. by P.O. Moore (American Society for Nondestructive Testing, Columbus, 2005)
8. J.H. Kurz, S. Köppel, L. Linzer, B. Schechinger, C.U. Grosse, in *Acoustic Emission Testing, Chap. 6: Source Localization*, ed. by C.U. Grosse, M. Ohtsu (Springer, Berlin, 2008), p. 101
9. S. Holland, T. Kosel, R. Weaver, W. Sachse, Ultrasonics **38**, 620 (2000)
10. J. Pujol, Seismol. Res. Lett. **75**, 63 (2004)
11. P.R. Murray, R.J. Dewhurst, Meas. Sci. Technol. **12**, 1651 (2001)
12. A.V. Smith, B.T. Do, Appl. Opt. **47**, 4812 (2008)
13. J.-D. Aussel, J.-P. Monchalin, Ultrasonics **27**, 165 (1989)
14. N.N. Hsu, *NBSIR 85-3234* (National Bureau of Standards, Washington, 1985)
15. R.J. Dewhurst, D.A. Hutchins, S.B. Palmer, C.B. Scruby, J. Appl. Phys. **53**, 4064 (1982)